Development of the early Cambrian oryctocephalid trilobite *Oryctocarella duyunensis* from western Hunan, China

Tao Dai,[1]* Nigel C. Hughes,[2] Xingliang Zhang,[1] and Shanchi Peng[3]

[1]State Key Laboratory for Continental Dynamics, Shaanxi Key Laboratory of Early Life and Environments, Northwest University, Xian, 710069, P.R. China <daitao@nwu.edu.cn>, <xzhang69@nwu.edu.cn>
[2]Department of Earth and Planetary Sciences, University of California, Riverside, CA 92521, USA, and Geological Studies Unit, Indian Statistical Institute, 203 B.T. Road, Kolkata, 700108, India <nigel.hughes@ucr.edu>
[3]State Key Laboratory of Palaeobiology and Stratigraphy (Nanjing Institute of Geology and Palaeontology, CAS), Nanjing, Jiangsu, 210008, P.R. China <scpeng@nigpas.ac.cn>

Abstract.—Abundant articulated specimens of the oryctocarine trilobite *Oryctocarella duyunensis* from the lower Cambrian (Stage 4, Series 2) Balang Formation at the Bulin section in western Hunan Province, South China, permit the description of all meraspid degrees. The maximum number of thoracic segments observed in this collection is 11. Meraspid growth was accompanied by progressive and gradual change in overall form, and this animal showed an homonymously segmented trunk with variation in the number of pygidial segments during ontogeny. Such variation permits a variety of plausible explanations, but a model of successive instars defined by the number of thoracic segments, and in suborder by the number of pygidial segments, is highly unlikely to explain the growth pattern because it would result in the loss of trunk segments between some instars. Degree-based ontogenetic staging is compatible with the variation observed.

Introduction

Corynexochids are a major trilobite clade with representation both in the Cambrian and Ordovician evolutionary radiations of Trilobita, being found from lower Cambrian to Middle Devonian deposits. They are characterized by a fused hypostome and rostral plate (Rasetti, 1952; Fortey, 1990; Whittington, 1995, but also see Bergström et al., 2014). Ontogenies have been described for a number of corynexochide taxa (e.g., Walcott, 1916; Poulsen, 1958; Suvorova, 1964; Rasetti, 1967; Robison, 1967; Chatterton, 1971; Robison and Campbell, 1974; Öpik, 1982; Lu and Qian, 1983; McNamara and Rudkin, 1984; Fortey and Chatterton, 1988; Lee and Chatterton, 2003; Park and Choi, 2009). Occasionally, their ontogenies are represented by abundant articulated exoskeletons. This combination of putative monophyly, long stratigraphic range, and good ontogenetic representation justifies a series of detailed case studies of the development of individual corynexochid species because of the clade's potential for insights into how trilobite life cycles evolved at a relatively fine taxonomic scale. In particular, the abundance of articulated ontogenies for a number of early Cambrian corynexochids from South China permits exploration of how developmental schedules varied among contemporary and rather closely related species (e.g., McNamara et al., 2003, 2006; Dai et al., 2014, 2017; Hou et al., 2015; Lei, 2016; Du et al., 2020), and perhaps, as we suggest below, even within individual species. As opposed to the more traditional, typological approach necessitated where examples are few, these animals offer glimpses into the natural variability of

development. This paper is the first of a series on the ontogeny of *Oryctocarella duyunensis* from the Bulin section in western Hunan that will explore its growth dynamics. Herein we discuss the systematic and geological context of the occurrence and provide a descriptive account of its ontogeny as a foundation for the more quantitative approach of subsequent papers. Fundamental and unique features of its development are documented.

McNamara et al. (2003, 2006) conducted pioneering ontogenetic investigations into the development of seven oryctocephalid species from the Balang Formation at Balang, Guizhou Province, China: *Oryctocarella duyunensis* Qian, 1961 (which those authors considered to be *Arthricocephalus chauveaui* Bergeron, 1899); *Oryctocarella balangensis* Lu and Qian in Yin and Li, 1978 (considered by them to be *Arthricocephalus xinzhaiheensis* Qian and Lin in Lu et al., 1974a); *Arthricocephalus xinzhaiheensis* (considered to be *Arthricocephalus balangensis* Lu and Qian in Yin and Li, 1978); *Arthricocephalus chauveaui* (considered to be *Arthricocephalus pulchellus* Zhang and Qian in Zhang et al., 1980); *Balangia balangensis* Qian, 1961; *Changaspis elongata* Lee in Qian, 1961; and *Duyunaspis duyunensis* Zhang and Qian in Zhou et al., 1977. Of these seven ontogenies, that of *Oryctocarella duyunensis* was one of the two most complete. McNamara et al.'s (2003) analysis of the ontogeny of *Oryctocarella duyunensis* illustrated specimens from each meraspid degree up to degree 9, thus laying the foundation for a more detailed exploration presented in this and forthcoming papers.

Geological setting

Oryctocephalids inhabited relatively deep-water, outer shelf and upper slope facies and were widely distributed in such settings across the Cambrian world (Whittington, 1995). *Oryctocarella*

---

*Corresponding author

is not only widely distributed in South China (including south-eastern Guizhou, western Hunan, northern Jiangxi, northwestern Zhejiang, and eastern Jiangsu), but also occurs in northern Greenland and Siberia (Tomashpolskaya and Karpinski, 1961; Blaker and Peel, 1997; Yuan et al., 2006). On account of its worldwide occurrence, *O. duyunensis* plays an important role in correlating across different continents within the traditional late early Cambrian and thus carries potential utility for defining the traditional lower/middle Cambrian boundary (=Cambrian Stage 4, Series 2). Accordingly, the combination of abundant articulated specimens available from a relatively narrow stratigraphic interval and intraspecific variation in its segmentation schedule offers potential for examining geographic variation in developmental patterns not only within southern China, but also among collections made from different continents.

On the South China block, oryctocephalids occur in abundance in a band of dark mudstone facies, referred to as the Jiangnan Belt (Peng and Babcock, 2001), that represents the shelf-slope transition during Cambrian Stage 4 and the subsequent Wuliuan. The Balang Formation, which hosts the great majority of *O. duyunensis*, crops out sporadically within an area of ~15,000 km^2 in eastern Guizhou and western Hunan (Fig. 1). In some places it is ~300 m thick and constitutes a series of mudstones and siltstones differentiated most evidently by color and amounts of carbonaceous and carbonate material (Lei, 2016; Zhao et al., 2019; Du et al., 2020). The total range of *Oryctocarella duyunensis* within the Balang Formation is as much as 290 m (Zhao et al., 2019, fig 2; Du et al., 2020, fig. 1), and it also extends into the overlying Qingxudong Formation, but it is most common within an interval of ~150 m in the middle to lower part of the Balang Formation. The great majority of our collections were recovered from interbedded argillaceous, arenaceous, and calcareous mudstones in an interval only 4 m thick (Fig. 1) in the lower part of the Balang Formation at the Bulin section, 6.3 km northwest of Jiwei village, Huayuan County, Hunan Province, South China (GPS coordinates 28.355°N, 109.384°E). Biostratigraphically, these fossils occur in Cambrian Series 2, Stage 4, depending on how the boundary between those stages is ultimately defined (Zhao et al., 2019, fig. 2), and possibly also in Stage 3.

Due both to the fine scale of bedding in these deposits, which makes tracing an individual bedding surface along strike difficult, and the fact that many beds contain fossils, to date many collections made for ontogenetic analysis of Balang Formation trilobites have paid limited attention to recording exactly where in the section specimens studied originated. This limits our ability to infer possible controls on patterns of variation witnessed within the sample (see Hughes et al., 2020). For example, several studies have recognized different meraspid "morphs" of the same degree based on different numbers of pygidial axial rings (e.g., Dai et al., 2017; Du et al., 2020), but we cannot determine if these occurred at all or only some of the stratigraphic levels sampled. Nevertheless, the studies of trilobites and other fossils from the Balang Formation reveal some level of consistency in preservational features among the beds. Specimens occur along bedding planes, and are usually partially or completely articulated. While they are quite common along certain bedding surfaces, the distribution of individuals along bedding planes appears overall to be sporadic, without the distinctive clustering seen in some later trilobite assemblages (e.g., Hughes and Cooper, 1999; Karim and Westrop, 2002). The density of specimen occurrence varies among bedding planes, but *O. duyunensis* and other trilobites are common at many levels in the formation.

Materials and methods

Herein we adopt suggestions for a methodological standard in the description of articulated trilobite ontogeny as recommended by Hughes et al. (2020). The fossils were photographed with a Canon 5Ds Digital SLR camera equipped with a Canon EF-S 60 mm 1:2.8 macro lens, in lower-angle lighting from the northwest direction and higher-angle lighting from the northeast direction, or, for the specimens smaller than 5 mm in length, with a Leica M205C stereomicroscope with a Planapo 1.0X lens, and the associated Leica Application Suite v. 4.10 software.

Materials.—More than 1700 specimens of *O. duyunensis*, including 1276 complete specimens, were recovered during fieldwork in 2012–2014. Of these complete specimens, various subsets were identified for particular analyses (see below). A detailed taphonomic analysis of trilobite distribution in the Balang Formation has yet to be conducted, but articulated specimens are found both in dorsal-up and dorsal-down positions along individual bedding surfaces. While isolated sclerites do occur, the majority of specimens are articulated, although not all are complete (Figs. 2.6, 6.1). Rarely, specimens are preserved in which the free cheeks and attached hypostome has swung beneath the cranidium, resulting in an inverted position facing posteriorly, and situated beneath the anterior part of trunk (Figs. 3.9, 4.1). Whittington (1990) made convincing arguments that this posture likely represents the result of molting behavior. Quite a number of specimens are also "axial shields" (sensu Henningsmoen, 1975) with free cheeks, and apparently also hypostomes, absent (e.g., Figs. 2.6, 3.9, 6.1, 6.3, 6.5, 6.8, 6.9). These may represent exuviae, but could result from post mortem sclerite displacement. On the other hand, many specimens of complete dorsal shields appear to have all sclerites in place (and include cracks in the glabella indicating that the hypostome was in position during compaction (e.g., Figs. 3.2, 3.6, 4.5–4.8, 5.1, 5.3, 5.5, 5.8, 5.9, 6.2, 6.7). Some of these likely represent carcasses, although an exuvium could possibly assume the appearance of a completely articulated exoskeleton on burial (Whittington, 1990). There is no indication of mechanical sorting of any of sclerite associations.

Measurements.—All dimensions were measured in mm as straight-line distances, and the measurements of the sagittal length are made from the anterior cranidial margin to the posterior pygidial margin.

Repository and institutional abbreviation.—All described and illustrated specimens are deposited in the paleontological collections of the Geology Department of Northwest
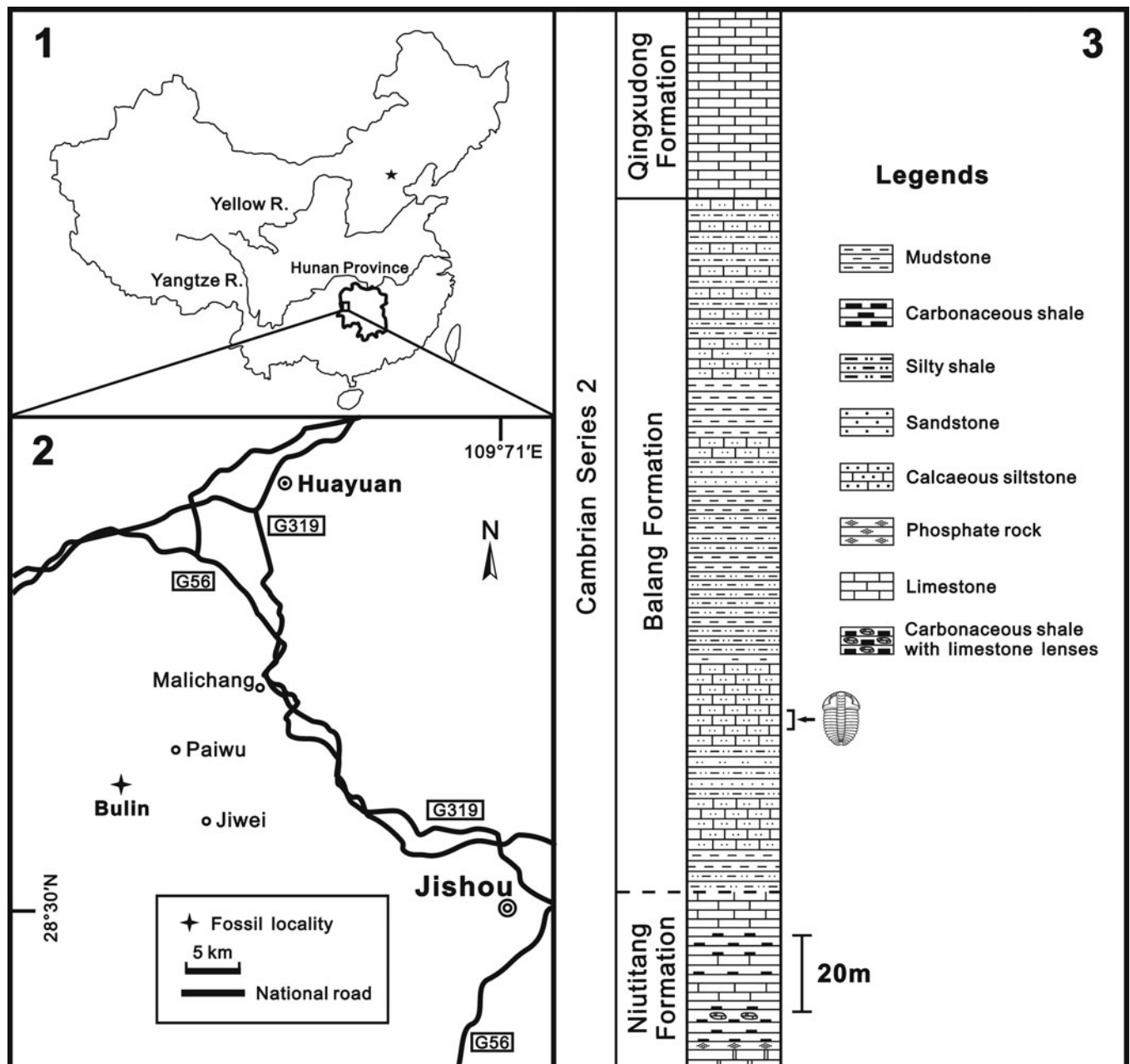
Figure 1. (**1**) Map of the People's Republic of China, showing the position of the collecting locality in western Hunan Province. (**2**) Sketch map of the fossil locality, Bulin section, ~6.3 km northwest of Jiwei village, Huayuan County, Hunan Province, South China. (**3**) Stratigraphic column of the Balang Formation (Stage 4, Series 2 of the Cambrian), with the arrow showing the 4 m thick stratigraphic interval in which the *O. duyunensis* collection studied herein was concentrated. As at other localities, *O. duyunensisi* occurs sporadically throughout much of this formation in this section.

University, Xi'an, China as part of the NWU-DYXJT 0001–1710 series.

Systematic paleontology

Terminology.—The morphological terms and abbreviations used in this paper follow Whittington and Kelly (1997). Abbreviations used in the descriptions include: exs. = exsagittal; LA = frontal glabellar lobe; sag. = sagittal; tr. = transverse; T = thoracic segment; T1–T11 = the first to the eleventh thoracic segment

from anterior to posterior, respectively; D0–D11 = degrees 0 to 11, respectively.

Order Corynexochida Kobayashi, 1935
Suborder Corynexochina Kobayashi, 1935
Family Oryctocephalidae Beecher, 1897

Remarks.—This group is characterized by a distinctive, pit-like structure of the glabellar furrows (Raymond, 1913), although not all taxa commonly assigned to the group possess this feature.
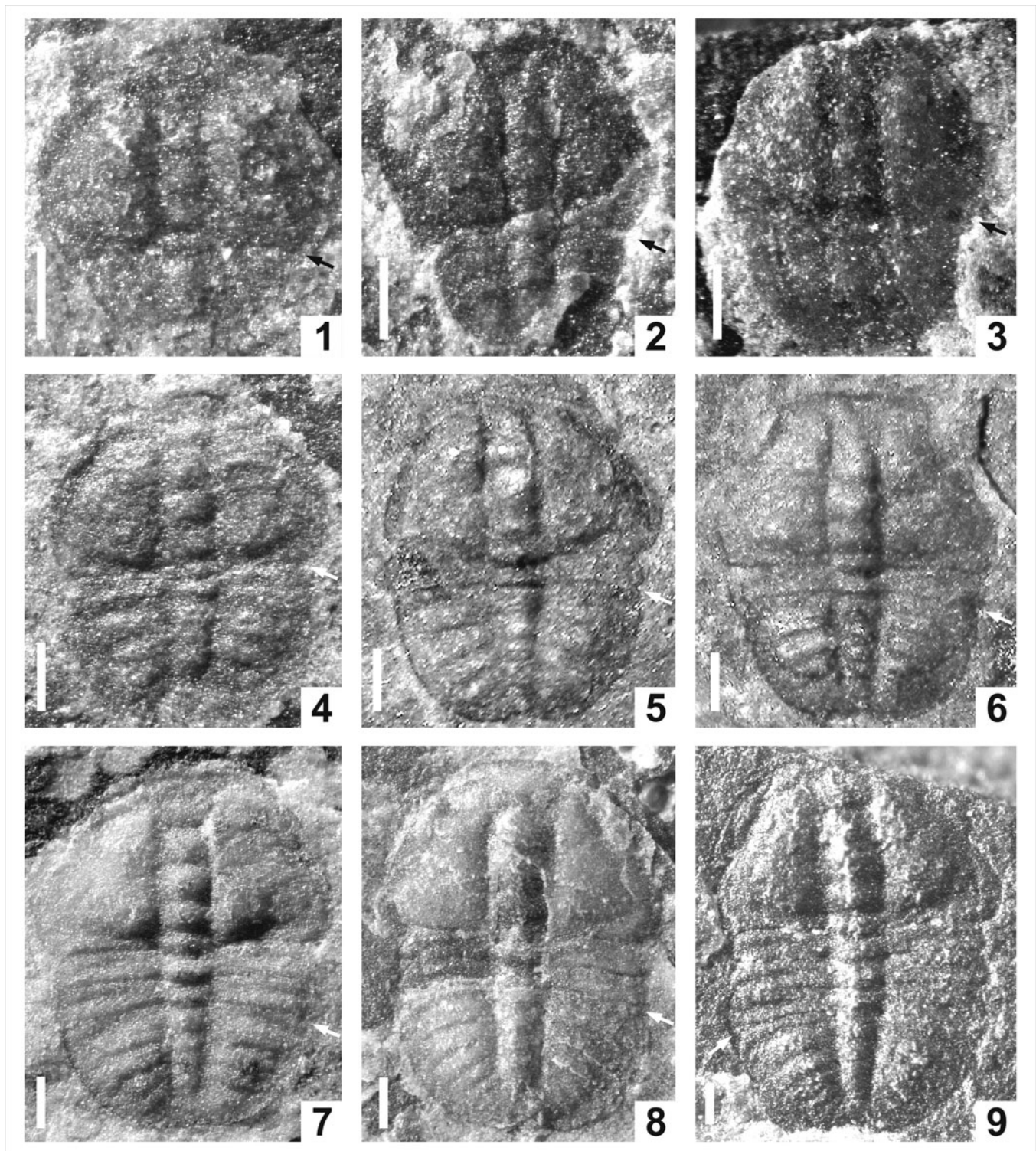
Figure 2. Complete meraspids of *Oryctocarella duyunensis* (Qian, 1961) from the Cambrian Stage 4 Balang Formation, Huayuan County, western Hunan Province, South China. (**1–3**) Degree 0; (**1**) m0,2 morph with two pygidial segments (NWU-DYXJT 0878), (**2, 3**) m0,5 morph with five pygidial segments (NWU-DYXJT 0460, NWU-DYXJT 2091). (**4–6**) Degree 1; (**4**) m1,5 morph with five pygidial segments (NWU-DYXJT 0046), (**5, 6**) m1,6 morph with six pygidial segments (NWU-DYXJT 2021, NWU-DYXJT 1596). (**7, 8**) Degree 2; (**7**) m2,5 morph with five pygidial segments (NWU-DYXJT 0009), (**8**) m2,6 morph with six pygidial segments (NWU-DYXJT 0407). (**9**) Degree 3; m3,5 morph with five pygidial segments (NWU-DYXJT 0693). Scale bars = 0.2 mm. Arrows indicate the boundary between cephalon or thorax and pygidium.

Phylogenetic relationships within the group have been considered recently (Whittington, 1995; Sundberg and McCollum, 1997; Sundberg, 2006, 2014; Peng et al., 2018), with the group traditionally divided phenetically into those animals with prominent marginal spines (Oryctocephalinae) and those without (Oryctocarinae and cheiuroids). Oryctocarinae generally share the
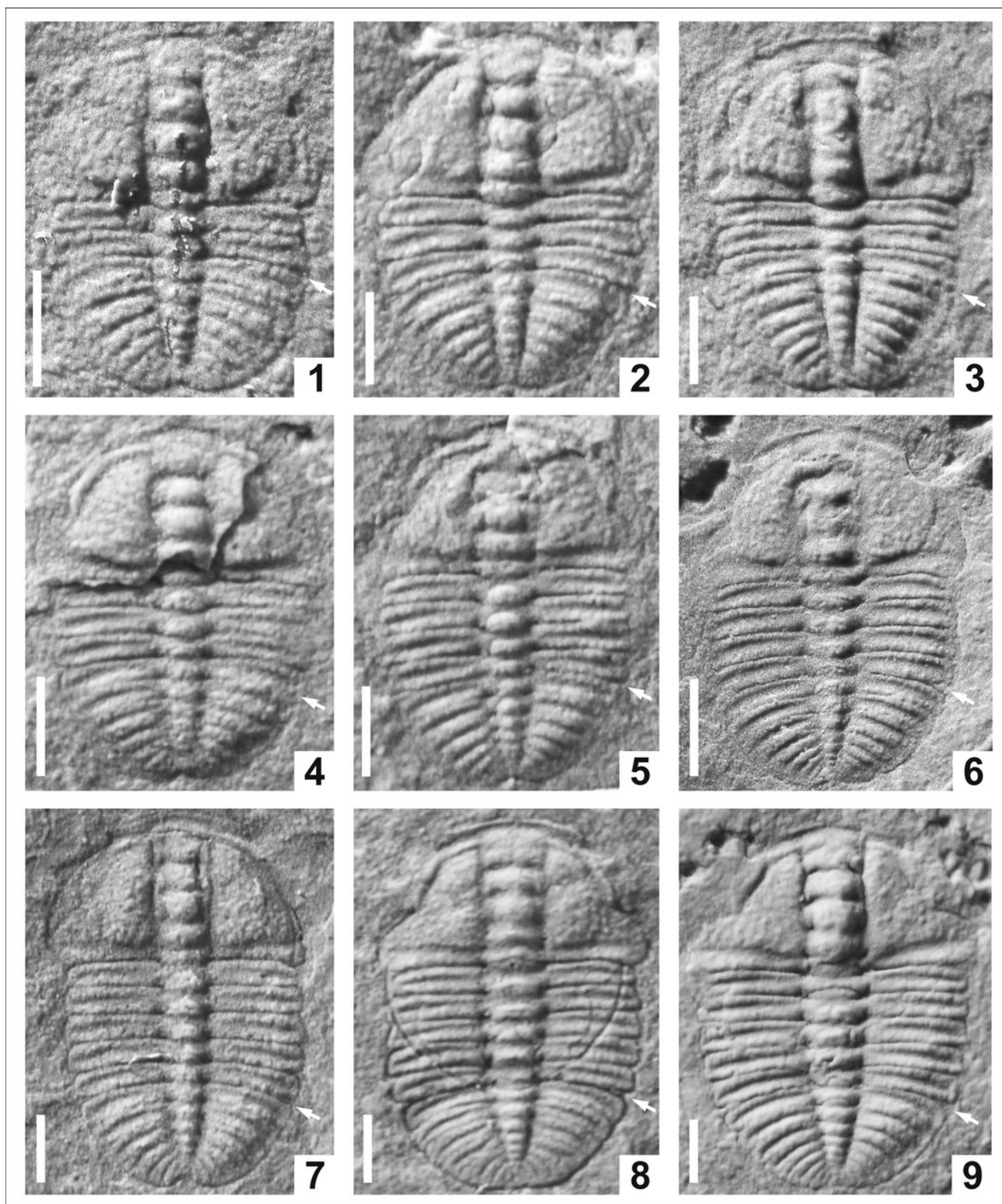
Figure 3. Complete meraspids of *Oryctocarella duyunensis* (Qian, 1961) from the Cambrian Stage 4 Balang Formation, Huayuan County, western Hunan Province, South China. (**1**) Degree 2; m2,7 morph with seven pygidial segments (NWU-DYXJT 1382). (**2, 3**) Degree 3; (**2**) m3,6 morph with six pygidial segments (NWU-DYXJT 0688), (**3**) m3,7 morph with seven pygidial segments (NWU-DYXJT 1206). (**4–6**) Degree 4; (**4**) m4,5 morph with five pygidial segments (NWU-DYXJT 1114), (**5**) m4,6 morph with six pygidial segments (NWU-DYXJT 1405), (**6**) m4,7 morph with seven pygidial segments (NWU-DYXJT 0383). (**7–9**) Degree 5; (**7**) m5,5 morph five pygidial segments (NWU-DYXJT 1130), (**8**) m5,6 morph with six pygidial segments (NWU-DYXJT 1216), (**9**) m5,7 morph with seven pygidial segments (NWU-DYXJT 0475). Scale bars = 0.5 mm. Arrows indicate the boundary between thorax and pygidium.

pit-like glabellar furrows with the spiny Oryctocephalinae, whereas cheiruroids do not. Sundberg (2006) considered whether Oryctocarinae and cheiruroids might root within the spiny Oryctocephalinae, and found a solution (Sundberg, 2006, fig. 2) in which cheiruroids were sister taxa to a larger group that included Oryctocarinae and Oryctocephalinae. This placement for Oryctocarinae was consistent with McNamara et al.'s (2006) view that this group rooted within Oryctocephalinae. However, based on their long branch lengths, Sundberg (2006, p. 65–66) rejected the placements of both Oryctocarinae and cheiruroids that his analysis suggested, but did not evaluate alternatives (such as whether Oryctocarinae and/or cheiruroids are sister taxa to all Oryctocephalinae), partly due to the difficulty of identifying a suitable outgroup assessing basal corynexochid relationships.

We find the phylogeny shown by Sundberg (2006, fig. 2) interesting in that it placed oryctocarine trilobites in a more crownward position than cheiruroids, and allied with members of the genus *Tonkinella*. In addition to its absent or greatly reduced marginal spines, *Tonkinella* is known for its reduced number of holaspid thoracic segments relative to spiny oryctocephalines, and has long been considered to be a paedomorphic form (Hupé, 1953; McNamara, 1986b, p. 139). More specifically, it has been considered progenetic (McNamara, 1986a) due to its reduced holaspid segment count and small size, both at onset of trunk maturity and at its maximum size observed. These features suggest an abbreviated or condensed ontogeny compared to that of its putative oryctocephaline ancestors. Such features also characterize oryctocarine and cheiruroid trilobites when compared to sister taxa among oryctocephalines (Sundberg, 2014), and so a dominantly progenetic origin might have applied to all. This would explain both convergence in form among them, and their marked phenetic differences from spiny forms (and thus long branch lengths). Hence, while we agree with Sundberg (2006, 2014) that relationships among these taxa are far from being confidently resolved, and have some reservations about heterochronic accounts of trilobite phylogeny (Webster et al., 2001; Hunda et al., 2006), the conclusion that processes broadly defined as progenetic played a role in many oryctocarine characters appears reasonable. Whatever oryctocarine sister taxon is ultimately resolved, it was apparently larger and possessed more trunk segments at maturity than any oryctocarine.

<div style="text-align:center">

Subfamily Oryctocarinae Hupé, 1953
Genus *Oryctocarella* Tomashpolskaya and Karpinski, 1961

</div>

Type species.—*Oryctocare siberica* Tomashpolskaya in Khalfin, 1960.

<div style="text-align:center">

Oryctocarella duyunensis (Qian, 1961)
Figures 2–6

</div>

1961 *Arthricocephalus duyunensis* Qian (part), p. 97, pl. 1, fig. 19, pl. 2, figs. 5, 7, 8, 10, ?fig. 9; non pl. 1, fig. 20, pl. 2, fig. 6.
         For synonymy up to 2017 see Peng et al. (2017, p. 951).

2019 *Oryctocarella duyunensis* (Qian, 1961); Zhao et al., fig. 3b, e.
2020 *Arthricocephalus chauveaui* Bergeron, 1899; Du et al., figs. 3–5.

Holotype.—Incomplete exoskeleton NIGP 11484 (Qian, 1961, pl. 2, fig. 8) from the Balang Formation, Duyun, eastern Guizhou, South China.

Remarks.—There has been recent debate about the correct name for the species considered herein. Some authors have applied the name *A. chauveaui* (e.g., Zhou et al., 1977; Zhang et al., 1980; Blaker and Peel, 1997; McNamara et al., 2003; Yuan et al., 2006, Du et al., 2020) to fossils from the Balang Formation that we consider belong to *Oryctocarella duyunensis*. Bergeron (Bergeron, 1899) first described *A. chauveaui* based on the material collected by M. Chauveau from the lower Cambrian Balang Formation in Tongren County, Guizhou Province, China. It differs notably from *Oryctocarella* by possessing an anteriorly expanded rather than cylindrical (or parallel-sided) glabella, glabellar furrows that are connected with dorsal furrows, fewer mature thoracic segments (8), and a larger pygidium that is almost equal in length and area to the cranidium (see Peng et al., 2015, 2017 for a detailed consideration of these issues). On the basis of an error in the published specimen number of the lectotype published in the 1980s, Du et al. (2020) continued to apply the name *A. chauveaui* to what is here considered to be *O. duyunensis*, but without providing reasoning as to why the acknowledged error should be further perpetuated. Here we use *Oryctocarella duyunensis* following the arguments of Peng et al. (2017).

Ontogeny

Of the 1276 complete specimens of *O. duyunensis*, 968 permitted measurement of their sagittal dorsal length. These vary from 0.65 to 10.20 mm in length and constitute what we refer to as "dataset 1." In 643 of these specimens, the segment number in both the thorax and pygidia can be counted with confidence: this is "dataset 2" (Figs. 2–6) (see Supplementary Material for summary statistics on these dataset). Here we recognize a series of degrees based on the number of thoracic segments, that include morphs (m) determined by the number of segments in the pygidium. While these degrees are defined by the number of thoracic segments, they are not all necessarily meraspid degrees. The notation m2,5 indicates a specimen with two thoracic segments and five axial rings in the pygidium (including the terminal piece). An extensive description of degree 9 is given rather than of degree 11, the form with the most thoracic segments, because degree 9 is numerically the most abundant form.

Degree 0.—Exoskeleton 0.65–1.02 mm in length, represented by nine articulated specimens (Fig. 2.1–2.3). Based upon the available material, this degree can be subdivided into two morphs according to the number of segments in the pygidia.

Morph m0,2. Exoskeleton sub-circular in outline (Fig. 2.1), cephalon sub-elliptical in outline. Anterior margin curved

forward; anterior border indistinct. Glabella narrow and of low convexity, parallel-sided and slightly expanded forward, with frontal glabellar lobe (LA) reaching anterior border furrow; four pairs of conjoined glabellar furrows weakly impressed. Fixigena wide (tr.) and protuberant, twice width (tr.) of glabella. Occipital ring (LO) shorter (sag.) and wider (tr.) than L1, with posterior margin slightly curved backward. Facial suture indistinct. Eye ridge and palpebral lobe weakly defined. Posterior border furrow weakly defined. Genal angle obtuse. Trunk small, semi-elliptical in outline, with posterior margin concave medially. Axis narrow (tr.) and poorly segmented, probably with 2–3 segments, with posterior tip close to posterior margin.

Morph m0,5. Exoskeleton sub-elliptical in outline (Fig. 2.2, 2.3). Anterior margin slightly curved forward; anterior border narrow (sag., exs.). Glabella of moderate convexity. Posterior border furrow shallow. Pygidium proportionally larger than previous stage with the addition of new segments, semi-circular in outline; at least four or five axial segments can be defined.

Degree 1.—Exoskeleton 0.73–1.19 mm in length, represented by nine articulated specimens (Fig. 2.4–2.6). Cranidium semi-circular in outline. Anterior margin curved anteriorly; anterior border narrow and of uniform width (sag., exs.), curved laterally to palpebral lobe. Glabella narrow (tr.) from L1 to L3, and then slightly expanded anteriorly from L4 to LA, with anterior margin reaching anterior border furrow; glabellar furrows weakly impressed, S1–S3 transverse, conjoined, S4 shallow and extending anteromedially. Facial suture proparian, anterior branch short, strongly convergent forward, posterior branch extending posterolaterally. Eye ridge weakly defined, located anteriorly, close to anterior border; palpebral lobe narrow (tr.) and short (sag.). Fixigenal field protuberant. Posterior margin straight laterally and then curved anterolaterally to intersect lateral margin. Posterior border extremely narrow (exs.); posterior border furrow shallow, extending anterolaterally.

Thorax with one segment. Axial ring weakly defined by shallow axial furrows, notably narrower than pleurae. Pleurae moderately flat, of equal length (exs.) laterally, with pleural spine short and obtuse; pleural furrow shallow.

Pygidium semi-circular in outline, with posterior margin concave medially, W-shaped in outline. Axis narrow (tr.), segments weakly incised, tapering evenly backward, with posterior tip close to posterior border. Pleural furrow weakly impressed. Two morphs are recognized in this degree, with five (m1,5; Fig. 2.4) and six (m1,6; Fig. 2.5, 2.6) segments in the pygidia.

Degree 2.—Exoskeleton 1.02–1.92 mm in length, represented by 55 articulated specimens (Figs. 2.7, 2.8, 3.1). Cephalon semi-circular in outline. As for Degree 1, except eye ridge moderately well defined, extending from LA or S4 and then curved posterolaterally; palpebral lobe small and curved outward, with posterior tip opposite S1. Thorax with two segments. Axis of moderate convexity, defined by shallow axial furrows. Pleurae moderately flat, gently shorter (exs.) and narrower (tr.) from T1 to T2. Pygidium with anterior margin extending posterolaterally and posterior margin concave medially, W-shaped in outline. Pygidial border narrow, weakly defined by shallow border furrow. Three

morphs can be recognized, with five (m2,5; Fig. 2.7), six (m2,6; Fig. 2.8), and seven (m2,7; Fig. 3.1) segments in the pygidial axis.

Degrees 3–11.—Exoskeletons range from 1.38 to 10.20 mm in length (Figs. 2.9, 3.2–3.9, 4–5). In addition to the extra thoracic segments, morphological changes among the subsequent phases were subtle, consisting most obviously of a progressive decrease in the relative width of the fixigenae, increased curvature of the palpebral lobes, more firmly incised glabellar furrows, contraction of the pronounced posteromedial notch in the pygidium, along with relative lengthening of the postaxial margin compared to the axial length. Various morphs can be recognized in these degrees according to the number of pygidial segments.

Degree 3.—Exoskeleton 1.43–2.13 mm in length, represented by 84 articulated specimens (Figs. 2.9, 3.2, 3.3). Thorax with three segments. Three morphs are recognized, with five (m3,5; Fig. 2.9), six (m3,6; Fig. 3.2), and seven (m3,7; Fig. 3.3) segments in the pygidium.

Degree 4.—Exoskeleton 1.38–3.19 mm in length, represented by 109 articulated specimens (Fig. 3.4–3.6). Thorax with four segments. Three morphs are recognized, with five (m4,5; Fig. 3.4), six (m4,6; Fig. 3.5), and seven (m4,7; Fig. 3.6) segments in the pygidium.

Degree 5.—Exoskeleton 1.71–3.82 mm in length, represented by 117 articulated specimens (Fig. 3.7–3.9). Thorax with five segments. Three morphs are recognized, with five (m5,5; Fig. 3.7), six (m5,6; Fig. 3.8), and seven (m5,7; Fig. 3.9) segments in the pygidium.

Degree 6.—Exoskeleton 2.13–4.42 mm in length, represented by 136 articulated specimens (Fig. 4.1–4.5). Thorax with six segments. Three morphs are recognized, with five (m6,5; Fig. 4.1, 4.2), six (m6,6; Fig. 4.3, 4.4), and seven (m6,7; Fig. 4.5) segments in the pygidial axis.

Degree 7.—Exoskeleton 2.89–5.05 mm in length, represented by 165 articulated specimens (Fig. 4.6–4.9). Thorax with seven segments. Two morphs are recognized, with five (m7,5; Fig. 4.6, 4.7) and six (m7,6; Fig. 4.8, 4.9) segments in the pygidium.

Degree 8.—Exoskeleton 3.31–7.81 mm in length, represented by 268 articulated specimens (Fig. 5.1–5.3). Thorax with eight segments. Two morphs are recognized, with four (m8,4; Fig. 5.1) and five (m8,5; Fig. 5.2, 5.3) segments in the pygidial axis.

Degree 9.—Exoskeleton 4.55–10.05 mm in length, represented by 288 articulated specimens (Fig. 5.4–5.9). Thorax with nine segments. Exoskeleton oval in outline. Cephalon semi-elliptical in outline, with granules preserved in some specimens. Cranidium sub-trapezoidal in outline. Anterior margin curved forward; anterior border extremely narrow (sag.) and upturned, of uniform width (sag., exs.) laterally to lateral border; anterior border furrow shallow. Glabella narrow, sub-cylindrical in outline, defined by deeply incised axial furrow; parallel-sided from L1 to L3, and then slightly expanded forward from L4 to LA; LA slightly expanded anteriorly and rounded in front, with anterior margin across anterior border furrow and reaching anterior border; S1–S3 pit-like, not extending to axial furrow, shallowing inward across middle of glabella; S4 short and shallow, extending slightly convergent and forward. Occipital ring
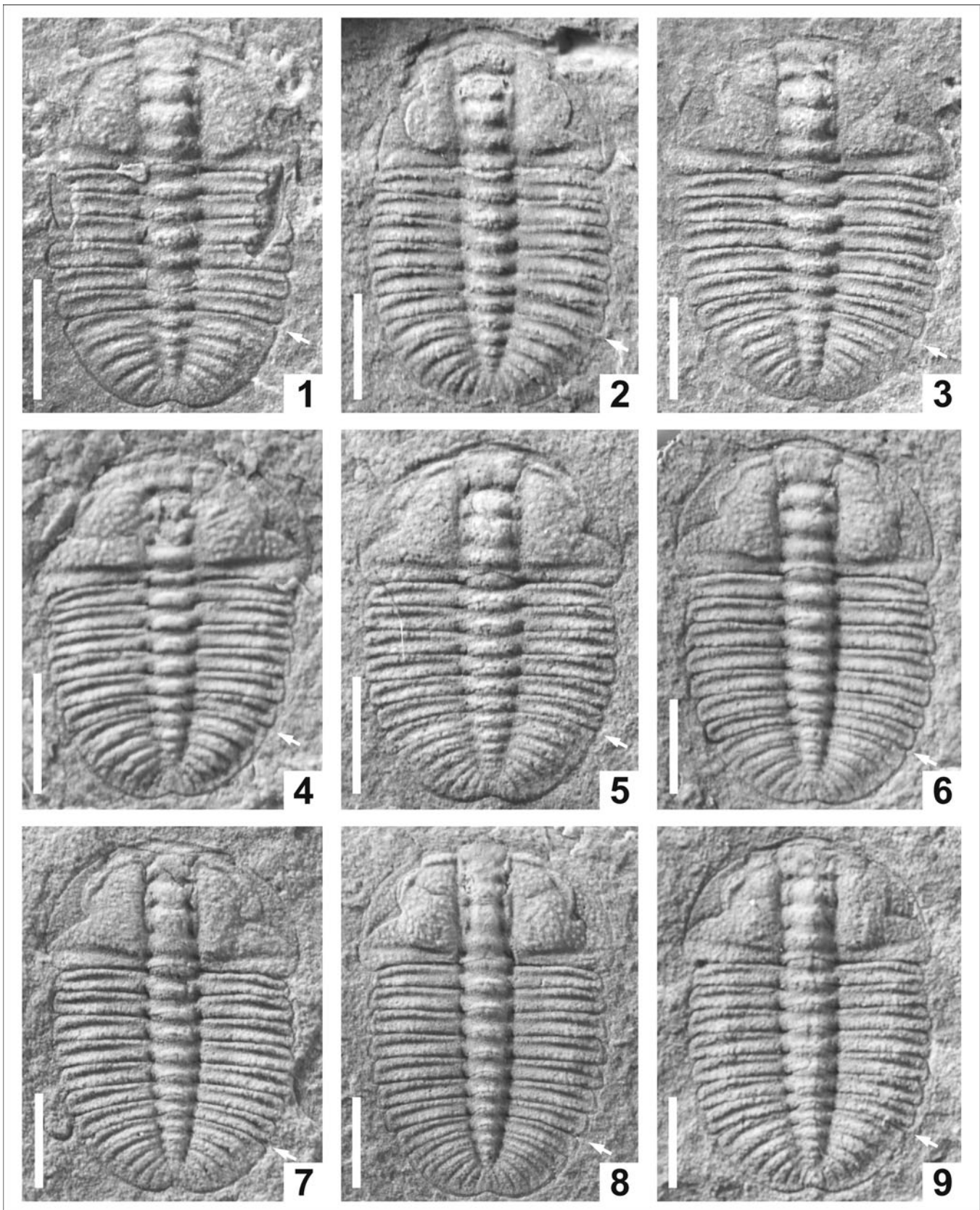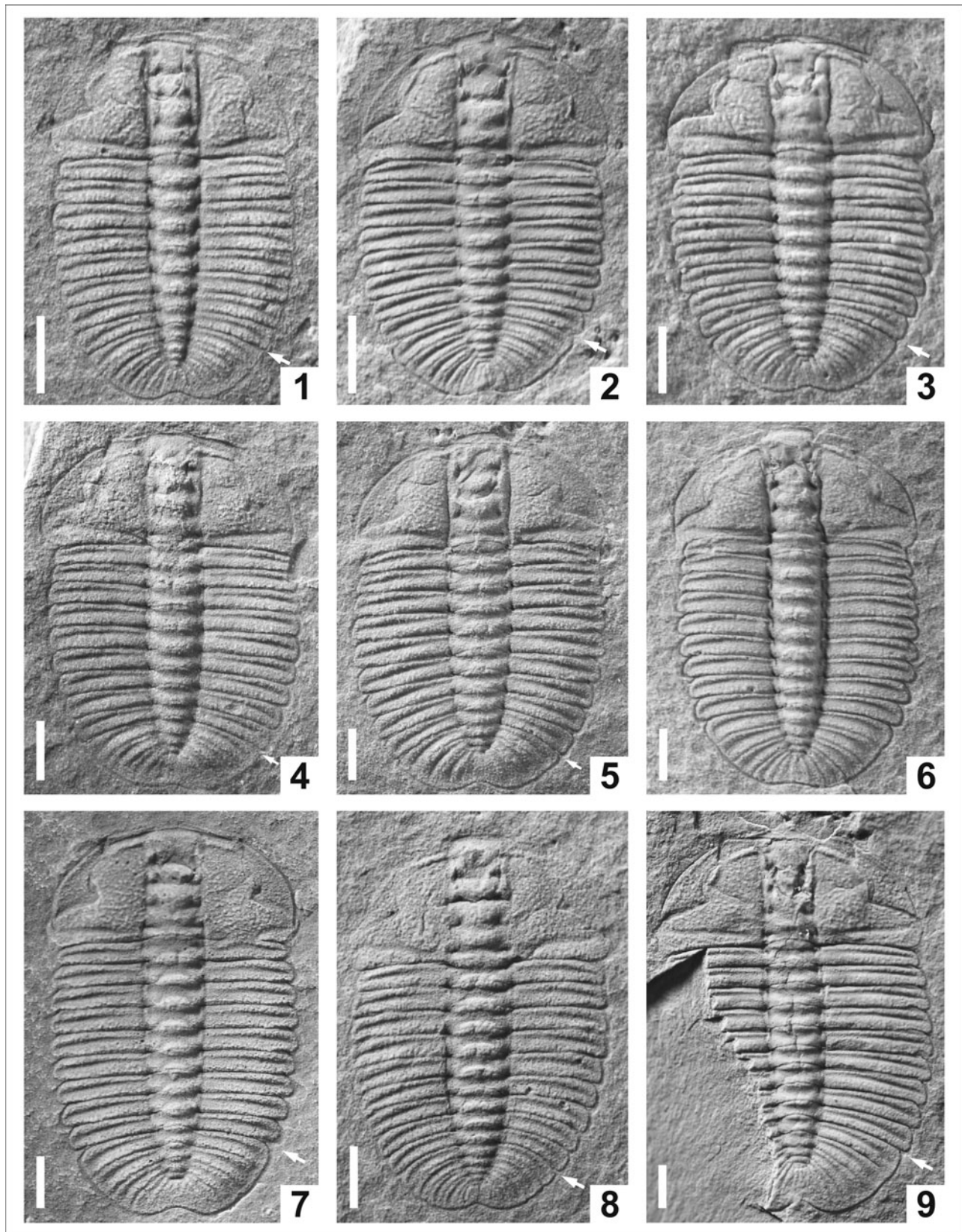
Figure 4. Complete meraspids of *Oryctocarella duyunensis* (Qian, 1961) from the Cambrian Stage 4 Balang Formation, Huayuan County, western Hunan Province, South China. (**1–5**) degree 6; (**1, 2**) m6,5 morph with five pygidial segments (NWU-DYXJT 0184, NWU-DYXJT 0540), (**3, 4**) m6,6 morph with six pygidial segments (NWU-DYXJT 0047, NWU-DYXJT 0418), (**5**) m6,7 morph with paven pygidial segments (NWU–DYXJT 0097). (**6–9**) Degree 7; (**6, 7**) m7,5 morph with five pygidial segments (NWU-DYXJT 1641, NWU-DYXJT 0304), (**8, 9**) m7,6 morph with six pygidial segments (NWU-DYXJT 0087, NWU-DYXJT 0533). Scale bars = 1 mm. Arrows indicate the boundary between thorax and pygidium.
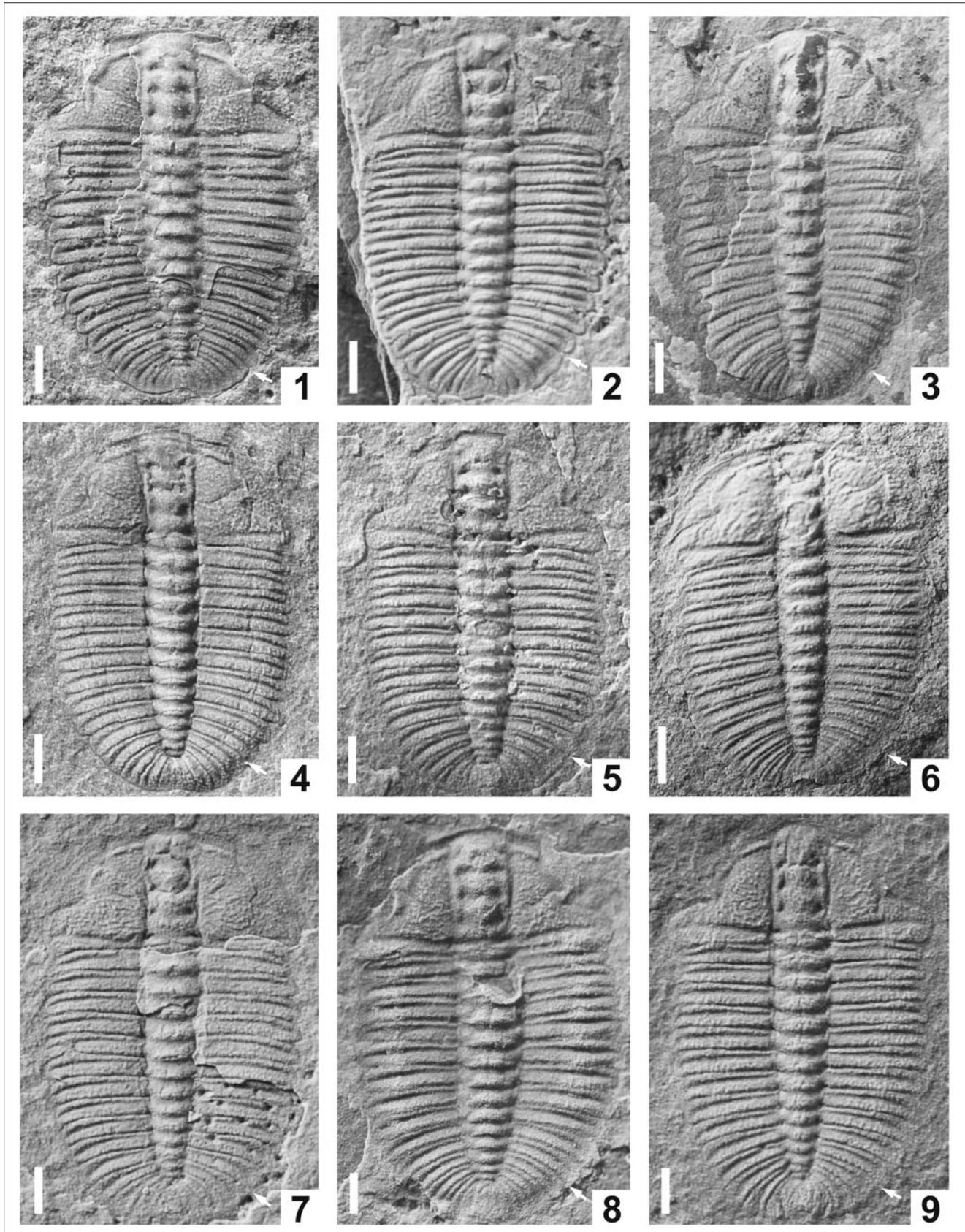
**Figure 5.** Larger articulated specimens of *Oryctocarella duyunensis* (Qian, 1961) from the Cambrian Stage 4 Balang Formation, Huayuan County, western Hunan Province, South China. (**1–3**) Degree 8; (**1**) m8,4 morph with four pygidial segments (NWU-DYXJT 1252), (**2, 3**) m8,5 morph with five pygidial segments (NWU-DYXJT 0572, NWU-DYXJT 1319). (**4–9**) Degree 9; (**4, 5**) m9,3 morph with three pygidial segments (NWU-DYXJT 1079, NWU-DYXJT 1294), (**6, 7**) m9,4 morph with four pygidial segments (NWU-DYXJT 1325, NWU-DYXJT 0876), (**8, 9**) m9,5 morph with five pygidial segments (NWU-DYXJT 1636, NWU-DYXJT 1607); (**9**) shows a leading pygidial segment that appears disarticulated in the axial region, but remains fused in the pleural region. Scale bars = 1 mm. Arrows indicate the boundary between thorax and pygidium.

Figure 6. Large articulated specimens of *Oryctocarella duyunensis* (Qian, 1961) from the Cambrian Stage 4 Balang Formation, Huayuan County, western Hunan Province, South China. (**1–6**) Degree 10; (**1–4**) m10,3 morph with three pygidial segments (NWU-DYXJT 1670, NWU-DYXJT 1434, NWU-DYXJT 0010, NWU-DYXJT 1980), (**5, 6**) m10,4 morph with four pygidial segments (NWU-DYXJT 1813, NWU-DYXJT 0003). (**7–9**) Degree 11 specimens, m11,3, with three pygidial segments (NWU-DYXJT 1823, NWU-DYXJT 1329, NWU-DYXJT 1282). Scale bars = 1 mm. Arrows indicate the boundary between thorax and pygidium.
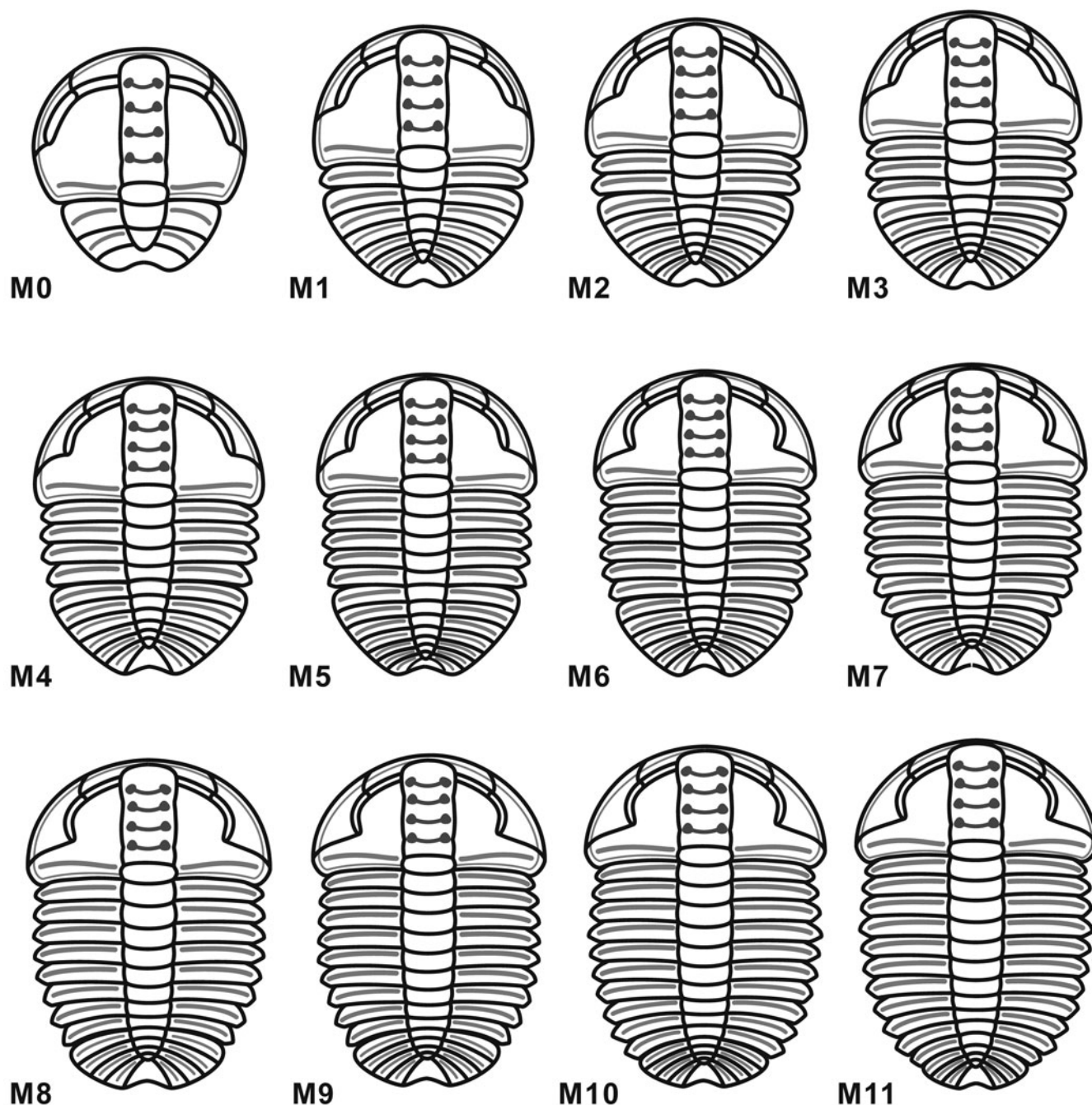
Figure 7. Reconstruction in dorsal view of the meraspid degrees of *Oryctocarella duyunensis* (Qian, 1961).

(LO) gently convex, shorter (sag.) and slightly wider (tr.) than transverse L1, with posterior margin curved backward, lacking an occipital spine or node; occipital furrow deeper abaxially and shallower adaxially, slightly curved backward. Eye ridge narrow and weakly defined, extending laterally from LA or S4, and then gently curved posterolaterally to palpebral lobe; palpebral lobe narrow, crescentic in outline, with anterior tip situated opposite L4 and posterior tip situated opposite L2. Facial suture proparian, anterior branches short, slightly convergent forward, cutting anterior border in a rounded curve.

Posterior margin extending laterally from axis curving slightly posterolaterally to genal angle. Posterior border wide (exs.) and convex, expanding abaxially; posterior border furrow shallow, extending anterolaterally. Fixigenal field broad, with maximum width across posterior border, twice width (tr.) of glabella. Librigena narrow in anterior portion and wider in posterior portion, lateral margin curved laterally.

Thorax with nine segments. Axis strongly narrower (tr.) than pleurae. Axial rings convex, defined by deeply incised axial furrows. Pleural lobe slightly convex (tr.), straight and parallel-sided
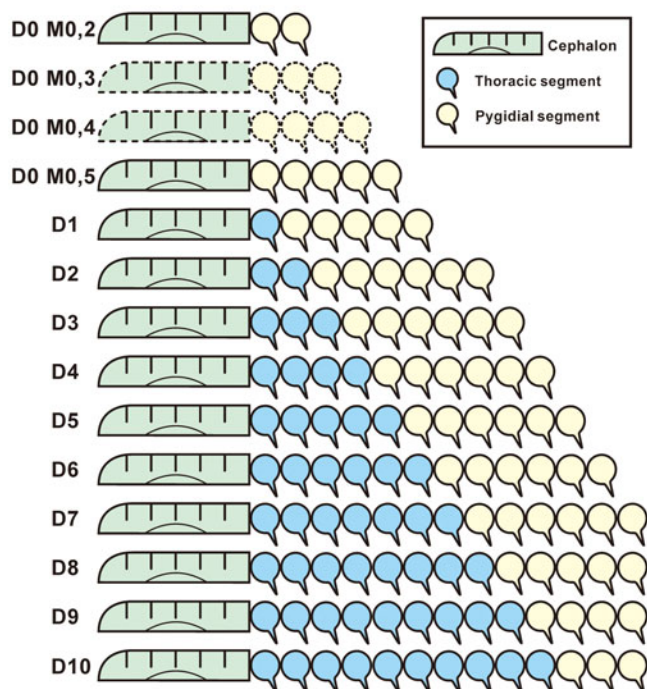
Figure 8. Trunk segmentation schedule for an individual of *Oryctocarella duyunensis* (Qian, 1961) from Bulin that is compatible with the observed changing mean number of segments allocated to the pygidium during meraspid ontogeny (see Fig. 9). The last instar in this individual is shown to have 10 thoracic segments, but this is not the case with all individuals in this sample. D represents "degree" and reflects the number of thoracic segments. Dotted lines represent forms hypothesized but not observed; gray, dark gray, and white represent cephalic, thoracic, and pygidial regions, respectively.

outward, and terminated in short and blunt pleural spines; pleural furrow shallow, located at anterior portion of the pleurae, extending to the end of pleural tip. Pleurae slightly wider (tr.) from T1 to T4 or T5, and then gently narrower (tr.) posteriorly from T5 to T9.

Pygidium, sub-elliptical in outline, with posterior margin concave medially. Axis narrow (tr.), tapering evenly backward, with posterior tip rounded and at a distance from posterior margin of about two fifths of pygidial length. Axial rings lacking spines, defined by shallow axial ring furrows, successively narrower (tr.) and shorter (sag.) posteriorly. Pleural field gently convex, defined by shallow border furrow. Anterior and posterior border narrow. Pleural ribs slightly curved posterolaterally, defined by distinct interpleural furrow; pleural furrow shallow and curved, extending to the end of pleural tip. Three morphs are recognized, with three (m9,3; Fig. 5.4, 5.5), four (m9,4; Fig. 5.6, 5.7), and five (m9,5; Fig. 5.8, 5.9) segments in the pygidial axis.

Degree 10.—Exoskeleton 5.36–10.20 mm in length, represented by 33 articulated specimens (Fig. 6.1–6.6). Body form largely as in degree 9. Thorax with 10 segments. Two morphs are recognized, with three (m10,3; Fig. 6.1–6.4) and four (m10,4; Fig. 6.5, 6.6) segments in the pygidial axis.

Degree 11.—Three articulated specimens assigned bearing 11 thoracic segments range in body length from 8.04 to 8.55 mm (Fig. 6.7–6.9). Body form largely as in degree 9. One morph recognized, with three segments in the pygidial axis (m11,4; Fig. 6.7–6.9).

Trunk segmentation schedule

The occurrence of multiple morphs within meraspid degrees contrasts with the ontogenetic scheme for this species reported by McNamara et al. (2003), in which they reported all degrees other than degree 3 had only one morph. In that study, the two morphs of meraspid degree 3 shared similar numbers of trunk segments, and differed only in size. Although McNamara et al. (2003) did not give details of their sample size, our analysis likely includes many more specimens. The presence of multiple morphs within meraspid degrees is supported by analysis of 216 specimens of the same species by Du et al. (2020) from the Lazizhai section, ∼9 km WSW of Balang. In their study, the multiple morphs within degrees included degree 0 (four morphs), degree 1 (three morphs), degree 3 (two morphs), degree 4 (two morphs), degree 6 (two morphs), and degree 8 (two morphs).

Our recognition of degrees and morphs is a descriptive one, and does not lead directly to any particular interpretation of ontogenetic stages and sequence. As in the case of many trilobite ontogenies, various alternative possibilities can explain the pattern of segment accretion and release observed in *O. duyunensis*. Du et al. (2020, fig. 9) proposed a model in which, within and between each meraspid degree, instars alternated with those in which a new segment was added to the pygidium, and those in which the leading pygidial segment was released into the thorax. Du et al.'s (2020, fig. 9) attractively crafted "trunk development schedule" suggests a steady and progressive increase in overall trunk proportions, but this obscures the alternating pattern of trunk segment addition and release that their model actually invokes. The pattern is similar to that suggested by Dai et al. (2014, fig. 6) for *Hunanocephalus ovalis* Lee in Egorova et al., 1963, which was also considered as one of the possibilities for the ontogeny of *Duodingia duodingensis* Chow in Lu et al., 1974b (see Hou et al., 2015, fig. 7A). However, as Hou et al. (2015, p. 508–511, fig. 7B, C) pointed out, other possible explanations exist for the same pattern.

Our study of *O. duyunensis* has an unusually large sample, and provides information on the relative abundances of the various morphs within meraspid degrees (Fig. 9). In terms of pygidial segment numbers, the median morph of degrees 2–6 and of degree 9, in each of which we recognize three morphs, consistently has the largest sample size. Among earlier meraspid degrees, in no case does any morph exceed 66% of the total number of specimens belonging to that degree, although one morph is always dominant. However, in degrees 7–10, one morph characterizes 75–85% of the sample. The data also show that within meraspid degrees, segment-rich morphs are generally larger than their segment-poor equivalents.

These observations alone are insufficient to discriminate with confidence among plausible developmental scenarios. However, the facts that three morphs are found within many of the degrees, and that some specimens of earlier degrees had more trunk segments than specimens of the subsequent degree, exclude applying the two successive instars per degree model of Du et al. (2020) to *O. duyunensis* from Bulin. This is not simply because there are commonly three, rather than two, morphs within a degree, but also because a strictly progressive interpretation of successive instars within a meraspid degree, based on
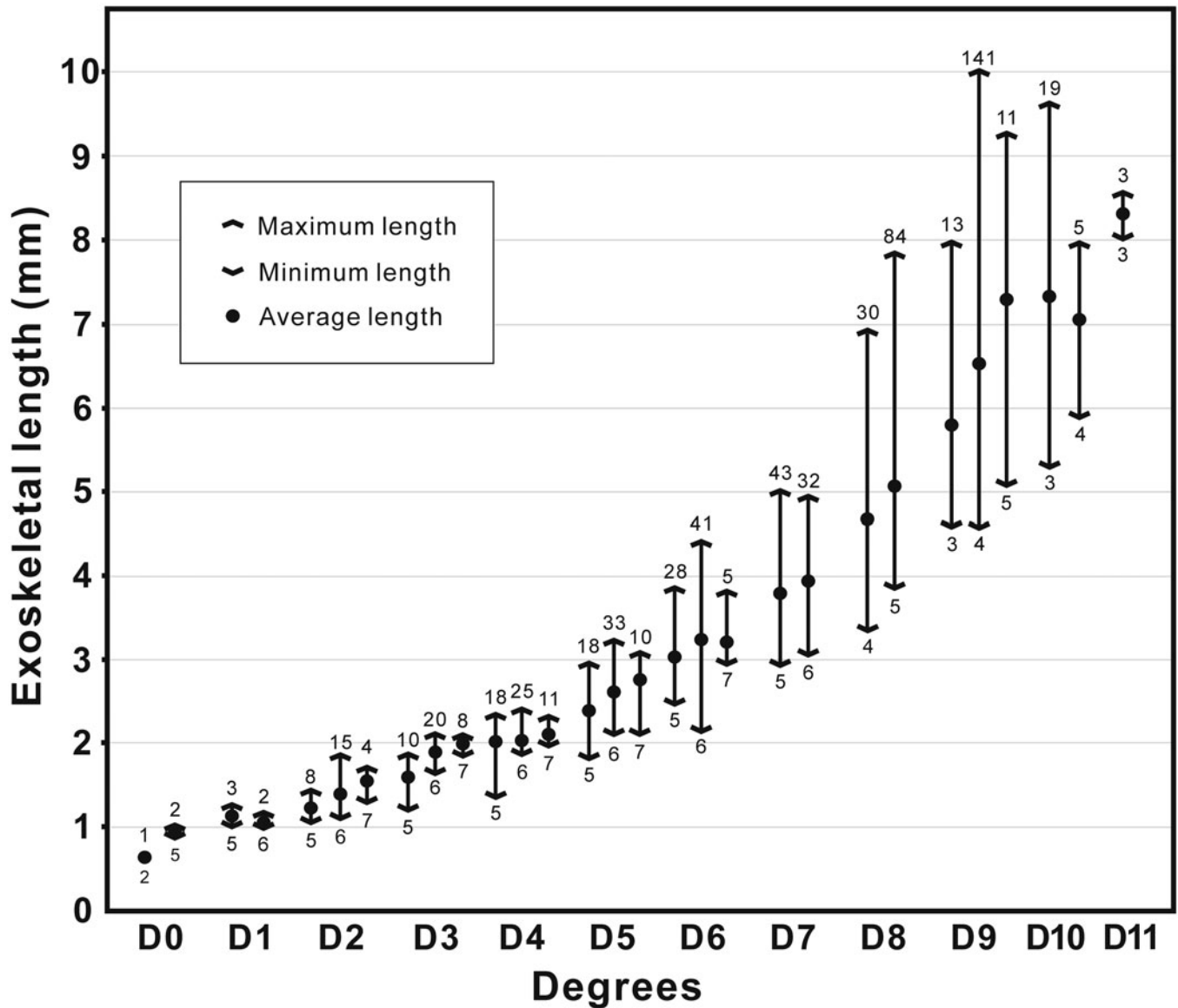
Figure 9. Meraspid exoskeletal lengths (including range and mean) in each degree and their associated morphs in *Oryctocarella duyunensis* (Qian, 1961), from dataset 2 (see text). The Arabic numerals above the arrowhead represent the number of specimens in which the trunk segments can be counted; Arabic numerals below the arrowhead represent the number of pygidial segments in the various morphs within each degree.

the number of pygidial segments (as proposed by Du et al., 2020) would require the number of trunk segments between successive degrees to have decreased, something unknown in living arthropods. Thus, it is highly unlikely that there were three successive instars within any meraspid degree of this animal beyond degree 0.

Phenotypic variance within the sample provides an alternative explanation for observed variation in number of pygidial segments expressed, with various types of phenotypic variation that might apply. For example, from degree 2 onwards, a possible interpretation of the data is the presence of three different morphotypes, each with a different number of pygidial segments at any given stage (Fig. 10). Alternatively, successive instars of the same individual trilobite might have shown different numbers of pygidial segments, even during the period of development in which pygidial segment accretion and release were in

balance (the "stasis phase" of Simpson et al., 2005) (also see Hou et al., 2015, 2017 for a similar discussion). The mean segment number of all specimens per degree summarizes the average degree-based ontogenetic pathway (Fig. 11), and the segmentation schedule presented for an individual of this species from this outcrop (Fig. 8) was constructed to conform closely to this average. With the observed early onset of variation in the number of pygidial segments, a variety of standard degree-based staging models is compatible with the data observed.

Discussion

The various ontogenetic schemes proposed above make different predictions about the patterns of size frequency distribution of individuals observed in the dataset, and these will be explored in forthcoming analyses. Pending these, our results can be
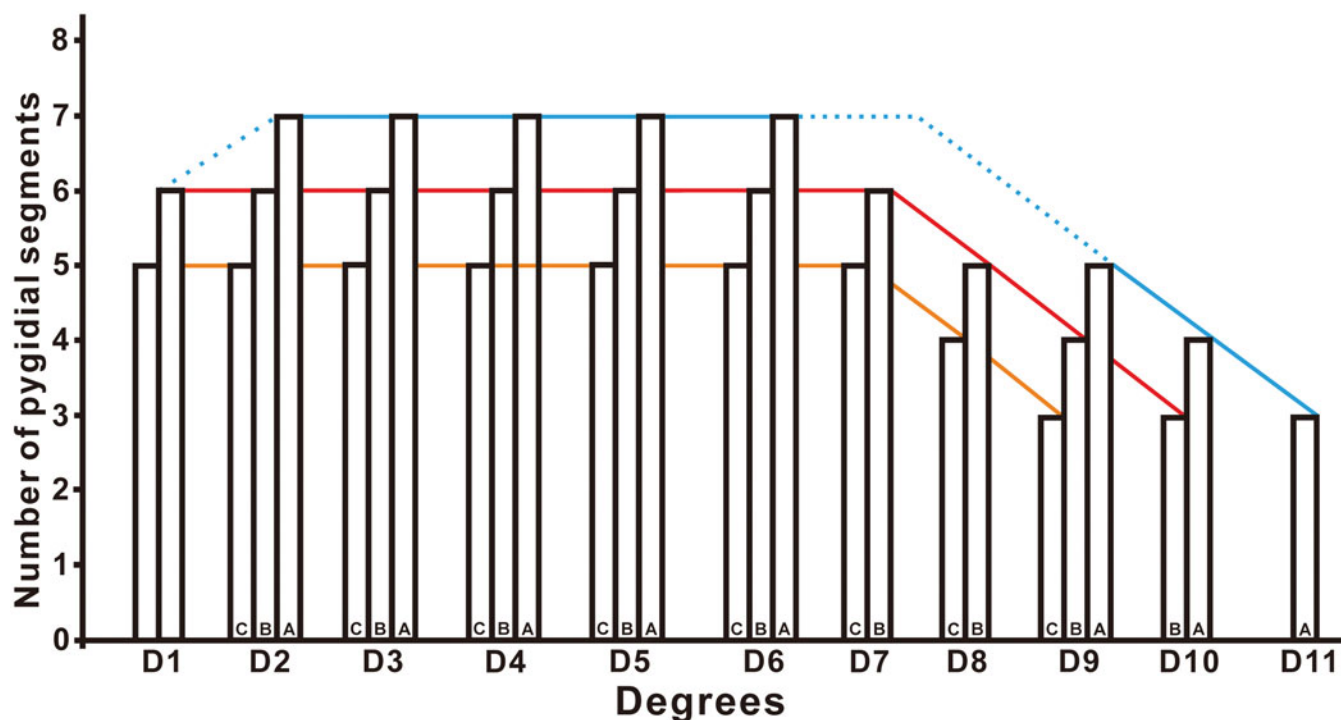
Figure 10. Hypothetical growth trajectories of three varieties of *Oryctocarella duyunensis*, one poor in pygidial segments (morphotype C), one rich in pygidial segments (morphotype A), and an intermediate form for degrees above degree 0 (morphotype B). Note that in this illustration, the onset of epimorphosis in all forms is at degree 7, and the ontogenetic pathway leading to degree 11 has two more instars than that leading to the segment-poor form of degree 9. Such a pattern of growth is consistent with the last three degrees (9–11) having progressively fewer morphs, and with the rising mean trunk number from degrees 9–11 as segment-poor morphs were progressively lost from the sample after the onset of epimorphosis at degree 7. The model predicts that additional morphs existed at D7 and D8 that were not captured in our sample, and is one among several ontogenetic pathways possible for this species.
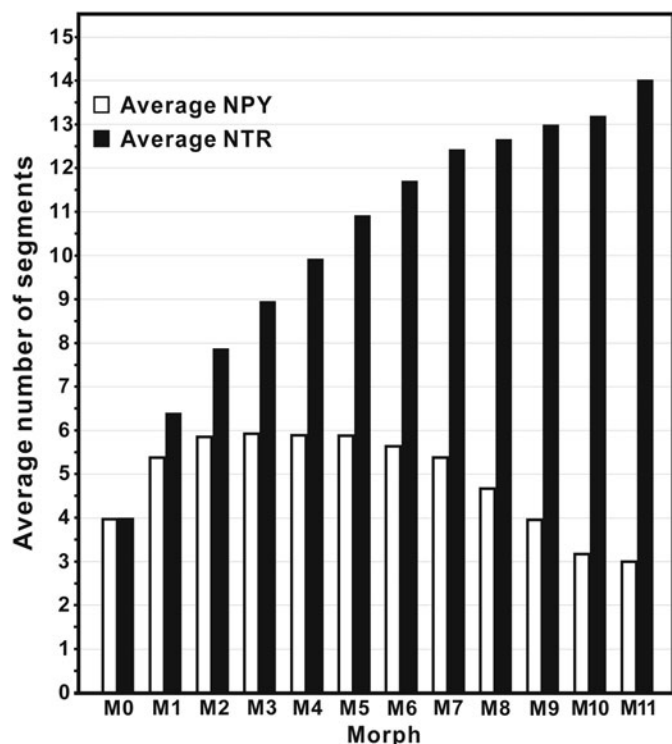

Figure 11. The mean numbers of trunk and pygidial segments for degrees of the Bulin *Oryctocarella duyunensis* (Qian, 1961). NPY = Number of pygidial axial rings, NTR = Number of trunk segments.

compared with those of Du et al. (2020) for the same species. Differences include the following: (1) the sizes of comparable degrees—in the Du et al. (2020) study "earlier" ontogenetic stages are consistently larger than those described herein (for example, degree 2 in this study varies from 1.02–1.92 mm in length, whereas in their study, degree 2 varies from 2.06–2.76); (2) the number of morphs present and distinguished in merapsid degree 0 is four in their study and only two in ours; (3) the constancy in number of segments in the merapsid pygidium after degree 0 in their study as opposed to the changing mean shown in ours; and (4) the onset of the holaspid phase at nine thoracic segments in their sample, as opposed to the 9–11 segments in our sample, representing a possible example of polymorphism. The latter observation in particular might provide grounds for distinguishing their sample and ours as different species, but we have not chosen this interpretation because other large specimens assigned to the same species from additional localities (including the type locality) are reported to bear many as 12 segments, suggesting a range of subtle ontogenetically related variation in mature segment numbers among collections (Peng et al., 2017, p. 951), rather than the appearance of novel morphologies per se.

We interpret this pattern to represent local intraspecific modification of ontogenetic mode, but acknowledge that such variation was likely the substrate for microevolutionary shifts in character states of a kind commonly associated with species-level distinction. Intraspecific variation in thoracic segment numbers is not uncommon, especially among Cambrian

and later trilobites with homonymous trunks (e.g., Hughes et al., 1999, 2017). What is more significant, perhaps, is the ability to observe such subtle differences in ontogenetic patterning among close relatives—something that is achieved quite rarely in studies of fossils (e.g., Webber and Hunda, 2007; Hopkins and Webster, 2009; Webster, 2015), and which offers a glimpse into the developmental basis for ancient microevolutionary change.

All *O. duyunensis* at Bulin apparently had a higher mean number of pygidial segments early in ontogeny than their conspecific relatives from the Lazizhai section in Guizhou, but converged on a similar number later in their ontogeny. If not an artefact of preservation, this may be a further example of the documentation of subtle patterns of developmental variance in ancient fossils.

A surprising aspect of the development of *O. duyunensis* at Bulin is the fact that the forms with the largest number of thoracic segments (degrees 10 and 11) span a relatively short range of sizes. Further work will explore the growth dynamics of the size and shape of this species in detail.

Acknowledgments

Accessibility of supplemental data

Data available from the Dryad Digital Repository: https://doi.org/10.5061/dryad.qfttdz0fn.

References

Beecher, C.E., 1897, Outline of a natural classification of the trilobites: American Journal of Science (ser. 4), v. 3, p. 89–106, 181–207.

Bergeron, J.N., 1899, Étude de quelques trilobites de Chine: Bulletin de la Société Géologique du France (Series 3), v. 27, p. 499–516.

Bergström, J., Zhou, Z., Alberg, P., and Axheimer, N., 2014, Upper lower Cambrian (provisional Cambrian Series 2) trilobites from northwestern Gansu Province, China: Estonian Journal of Earth Sciences, v. 63, p. 123–143.

Blaker, M.R., and Peel, J.S., 1997, Lower Cambrian trilobites from North Greenland: Meddelelser om Grønland, Geosciences, v. 35, p. 1–145.

Chatterton, B.D.E., 1971, Taxonomy and ontogeny of Siluro-Devonian trilobites from near Yass, New South Wales: Palaeontographica, Abteilung, v. 137, p. 1–108.

Dai, T., Zhang, X.-L., and Peng, S.-C., 2014, Morphology and ontogeny of *Hunanocephalus ovalis* (trilobite) from the Cambrian of South China: Gondwana Research, v. 25, p. 991–998.

Dai, T., Zhang, X.-L., Peng, S.-C., and Yao, X.-Y., 2017, Intraspecific variation of segmentation in the oryctocephalid trilobite *Duyunaspis duyunensis* from the Cambrian (Stage 4, Series 2) of South China: Lethaia, v. 50, p. 527–539.

Du, G.-Y., Peng, J., Wang, D.-Z., Wen, R.-Q., and Liu, S., 2020, Morphology and trunk development of the trilobite *Arthricocephalus chauveaui* from the Cambrian Series 2 of Guizhou, South China: Historical Biology, v. 32, p. 174–186.

Egorova, L.I., Xiang, L.W., Lee, S.J., Nan, R.S., and Guo, Z.M., 1963, The Cambrian trilobite faunas of Guizhou and western Hunan: Special Paper, Institute of Geology and Mineral Resources (Beijing), Series B, Stratigraphy and Palaeontology, v. 3, p. 1–117.

Fortey, R.A., 1990, Ontogeny, hypostome attachment and trilobite classification: Palaeontology, v. 33, p. 529–576.

Fortey, R.A., and Chatterton, B.D.E., 1988, Classification of the trilobite suborder Asaphina: Palaeontology, v. 31, p. 165–222.

Henningsmoen, G., 1975, Moulting in trilobites: Fossils and Strata, v. 4, p. 179–200.

Hopkins, M.E., and Webster, M., 2009, Ontogeny and geographic variation of a new species of the corynexochine trilobite *Zacanthopsis* (Dyeran, Cambrian): Journal of Paleontology, v. 83, p. 524–547.

Hou, J.-B., Hughes, N.C., Lan, T., Yang, J., and Zhang, X.-G., 2015, Early postembryonic to mature ontogeny of the oryctocephalid trilobite *Duodingia duodingensis* from the lower Cambrian (Series 2) of southern China: Papers in Palaeontology, v. 1, no. 4, p. 497–513.

Hou, J.-B., Hughes, N.C., Yang, J., Lan, T., Zhang, X.-G., and Dominguez, C., 2017, Ontogeny of the articulated yiliangellinine trilobite *Zhangshania typica* from the lower Cambrian (Series 2, Stage 3) of southern China: Journal of Paleontology, v. 91, p. 86–99.

Hughes, N.C., and Cooper, D.L., 1999, Paleobiologic and taphonomic aspects of the "*granulosa*" trilobite assemblage, Kope Formation (Upper Ordovician, Cincinnati region): Journal of Paleontology, v. 73, p. 306–319.

Hughes, N.C., Chapman, R.E., and Adrain, J.M., 1999, The stability of thoracic segmentation in trilobites: a case study in developmental and ecological constraints: Evolution & Development, v. 1, p. 24–35.

Hughes, N.C., Hong, P.S., Hou, J.-B., and Fusco, G., 2017, The development of the Silurian trilobite *Aulacopleura koninckii* reconstructed by applying inferred growth and segmentation dynamics: a case study in paleo-evo-devo: Frontiers in Ecology and Evolution, Evolutionary Developmental Biology, v. 5, article 37. https://doi.org/10.3389/fevo.2017.00037.

Hughes, N.C., Adrain, J.M., Holmes, J.D., Hong, P.S., Hopkins, M.J., Hou, J.-B., Minelli, A., Park, T.-Y.S., Paterson, J.R., Peng, J., Webster, M., Zhang, X.-G., Zhang, X.-L., and Fusco, G., 2020, Articulated trilobite ontogeny: suggestions for a methodological standard: Journal of Paleontology. https://doi.org/10.1017/jpa.2020.96.

Hunda, B.R., Hughes, N.C., and Flessa, K.W., 2006, Trilobite taphonomy and temporal resolution in the Mt Orab Shale Bed (Upper Ordovician, Ohio, USA): Palaios, v. 21, p. 26–45.

Hupé, P., 1953 [1952], Contribution a l'étude du Cambrien inférieur et du Précambrien III de l'Anti-Atlas Marocain: Division des mines et de la géologie, Service Géologique, Notes et Memoires, v. 103, p. 1–402.

Karim, T., and Westrop, S.R., 2002, Taphonomy and paleoecology of Ordovician trilobite clusters, Bromide Formation, south-central Oklahoma: Palaios, v. 17, p. 394–402.

Khalfin, L.L., ed., 1960, Biostratigrafiya Paleozoya Sayano-Altayskoy Gornoy Oblasti. Tom 1: Nizhniy Paleozoy [Biostratigraphy of the Paleozoic of the Sayan-Altai mountain range. Volume 1: Lower Paleozoic]: Trudy Sibirskogo Nauchno-Issledovatelskogo Instituta Geologii, Geofiziki i Mineralnogo Syrya, v. 19, p. 1–498. [in Russian]

Kobayashi, T., 1935, The Cambro-Ordovician formations and faunas of South Chosen. Palaeontology. Part 3. Cambrian faunas of South Chosen with a special study on the Cambrian trilobite genera and families: Journal of the Faculty of Science, Imperial University of Tokyo, Section II, v. 4, p. 49–344.

Lee, D.C., and Chatterton, B.D.E., 2003, Protaspides of *Leiostegium* and their implications for membership of the order Corynexochida: Palaeontology, v. 46, p. 431–445.

Lei, Q.-P., 2016, New ontogenetic information on *Duyunaspis duyunensis* Zhang & Qian in Zhou et al., 1977 (Trilobita, Corynexochida) from the Cambrian and its possible sexual dimorphism: Alcheringa, v. 40, p. 12–23.

Lu, Y.-H., and Qian, Y.-Y., 1983, Cambro-Ordovician trilobites from eastern Guizhou: Palaeontologia Cathayana, v. 1, p. 1–106. [in Chinese]

Lu, Y.H., Chang, W., Chien, Y., Chu, C., Lin, H., Zhou, Z., Qian, Y., Zhang, S., and Wu, H., 1974a, Cambrian trilobites, *in* Nanjing Institute of Geology and Palaeontology, ed., A Handbook of the Stratigraphy and Paleontology in Southwest China: Beijing, Science Press, p. 82–107. [in Chinese]

Lu, Y.H., Qian, Y.Y., Zhou, Z.Y., Qian, Y., Zhang, S.G., and Wu, H.J., 1974b, Bio-environmental control hypothesis and its application to the Cambrian biostratigraphy and palaeozoogeography: Memoir of the Nanjing Institute of Geology and Palaeontology, Academica Sinica, v. 5, p. 27–110. [in Chinese]

McNamara, K.J., 1986a, A guide to the nomenclature of heterochrony: Journal of Paleontology, v. 60, no. 1, p. 4–13.

McNamara, K.J., 1986b, The role of heterochrony in the evolution of Cambrian trilobites: Biological Reviews, v. 61, p. 121–156.

McNamara, K.J., and Rudkin, D.M., 1984, Techniques of trilobite exuviation: Lethaia, v. 17, p. 153–173.

McNamara, K.J., Yu, F., and Zhou, Z.-Y., 2003, Ontogeny and heterochrony in the oryctocephalid trilobite *Arthricocephalus* from the Early Cambrian of China: Special Papers in Palaeontology, v. 70, p. 103–126.

McNamara, K.J., Yu, F., and Zhou, Z.-Y., 2006, Ontogeny and heterochrony in the Early Cambrian oryctocephalid trilobites *Changasips*, *Duyunaspis* and *Balangia* from China: Palaeontology, v. 49, p. 1–19.

Öpik, A.A., 1982, Dolichometopid trilobites of Queensland, Northern Territory, and New South Wales: Bureau of Mineral Resources, Geology and Geophysics of Australia, Bulletin, v. 175, p. 1–85.

Park, T.Y., and Choi, D.K., 2009, Post-embryonic development of the Furongian (late Cambrian) trilobite *Tsinania canens*: implications for life mode and phylogeny: Evolution & Development, v. 11, p. 441–455.

Peng, S.-C., and Babcock, L.E., 2001, Cambrian of the Hunan-Guizhou Region, South China, *in* Peng, S.-C., Babcock, L.E., and Zhu, M.-Y., eds., Cambrian System of South China: Palaeoworld, v. 13, p. 3–51. http://english.nigpas.cas.cn/sp/Palaeoworldbackup/vol13/.

Peng, S.-C, Zhu, X.-J., Babcock, L.E., and Korovnicov, I.V., 2015, Restudy on the genus *Arthricocephalus* (Cambrian): concept and synonyms: Guizhou Geology, v. 32, p. 83–90.

Peng, S.-C., Babcock, L.E., Zhu, X.-J., Lei, Q., and Dai, T., 2017, Revision of the oryctocephalid trilobite genera *Arthricocephalus* Bergeron and *Oryctocarella* Tomashpolskaya and Karpinski (Cambrian) from South China and Siberia: Journal of Paleontology, v. 91, p. 933–959.

Peng, S.-C, Babcock, L.E., Zhu, X.-J., and Dai, T., 2018, A new oryctocephalid trilobite from the Balang Formation (Cambrian Stage 4) of northwestern Hunan, South China, with remarks on the classification of oryctocephalids: Palaeoworld, v. 27, p. 322–333.

Poulsen, V., 1958, Contribution to the palaeontology of the Lower Cambrian Wulff River Formation: Meddelelser om Grønland, v. 162, p. 1–25.

Qian, Y.-Y., 1961, Cambrian trilobites from Sandu and Duyun, southern Guizhou: Acta Palaeontologica Sinica, v. 9, p. 91–109.

Rasetti, F., 1952, Ventral cephalic sutures in Cambrian trilobites: American Journal of Science, v. 250, p. 885–898.

Rasetti, F., 1967, Lower and middle Cambrian trilobite faunas from the Taconic sequence of New York: Miscellaneous Collections of the Smithsonian Institution, v. 152, p. 1–111.

Raymond, P.E., 1913, Trilobita, *in* Eastman, C.R., ed., Text-book of Paleontology, 2nd Edition: London, Macmillan, v. 1, p. 692–729.

Robison, R.A., 1967, Ontogeny of *Bathyuriscus fimbriatus* and its bearing on the affinities of corynexochid trilobites: Journal of Paleontology, v. 41, p. 213–221.

Robison, R.A., and Campbell, D.P., 1974, A Cambrian corynexochid trilobite with only two thoracic segments: Lethtia, v. 7, p. 273–282.

Simpson, A.G., Hughes, N.C., Kopaska-Merkel, D.C., and Ludvigsen, R., 2005, Development of the caudal exoskeleton of the pliomerid trilobite *Hintzeia plicamarginis* new species: Evolution & Development, v. 7, p. 528–541.

Sundberg, F.A., 2006, Taxonomic assignment of the Cambrian trilobite *Tonkinella* Mansuy, 1916 (Corynexochida), with a new species from California: Memoirs of the Association of Australasian Palaeontologists, v. 32, p. 59–74.

Sundberg, F.A., 2014, Phylogenetic analysis of the spiny oryctocephalids (Trilobita, Corynexochida?, Oryctocephalidae), Cambrian: Journal of Paleontology, v. 88, p. 556–587.

Sundberg, F.J., and McCollum, L.B., 1997, Oryctocephalids (Corynexochida: Trilobita) of the lower-middle Cambrian boundary interval from California and Nevada: Journal of Paleontology, v. 71, p. 1065–1090.

Suvorova, N.P., 1964, The Corynexochida trilobites and their historical development: Proceedings of the Palaeontological Institute, Moscow, v. 103, p. 1–319. [in Russian]

Tomashpolskaya, V.D., and Karpinski, R.B., 1961, Some middle Cambrian trilobites from the region of village Sukhaya Erba (Batenevski Ridge): Izvestiya Tomsk Polytekhnik Instituta, v. 120, p. 152–160. [in Russian]

Walcott, C.D., 1916, Cambrian geology and paleontology III, no. 5: Cambrian trilobites: Smithsonian Miscellaneous Collections, v. 64, p. 303–457.

Webber, A.J., and Hunda, B.R., 2007, Quantitatively comparing morphological trends to environment in the fossil record (Cincinnatian Series; Upper Ordovician): Evolution, v. 61, p. 1455–1465.

Webster, M., 2015, Ontogeny and intraspecific variation of the early Cambrian trilobite *Olenellus gilberti*, with implications for olenelline phylogeny and evolutionary trends in phenotypic variation: Journal of Systematic Palaeontology, v. 13, p. 1–74.

Webster, M., Sheets, H.D., and Hughes, N.C., 2001, Allometric patterning in trilobite ontogeny: testing for allometric heterochrony in *Nephrolenellus*, *in* Zelditch, M.L., ed., Beyond Heterochrony: New York, Wiley-Liss, p. 105–144.

Whittington, H.B., 1990, Articulation and exuviation in Cambrian trilobites: Philosophical Transactions of the Royal Society of London, Series B, v. 329, p. 27–49.

Whittington, H.B., 1995, Oryctocephalid trilobites from the Cambrian of North America: Palaeontology, v. 38, p. 543–562.

Whittington, H.B., and Kelly, S.R.A., 1997, Morphological terms applied to Trilobita, *in* Kaesler, R.L., ed., Treatise on Invertebrate Paleontology, Part O, Arthropoda 1, Trilobita, Revised. Volume 1: Introduction, Order Agnostida, Order Redlichiida: Boulder, Colorado and Lawrence, Kansas, Geological Society of America and University of Kansas Press, p O313–O329.

Yin, G.Z., and Li, S.J., 1978, Trilobita, *in* Stratigraphical and Palaeontological Working Group of Guizhou Province, ed., Palaeontological Atlas of Southwest China, Guizhou Volume 1. Cambrian–Devonian: Beijing, Geological Publishing House, p. 385–594, 798–829. [in Chinese]

Yuan, J.-L., Zhao, Y.-L., and Yang, X.-L., 2006, Speciation of the genus *Arthricocephalus* Bergeron, 1899 (Trilobita) from the late early Cambrian and its stratigraphic significance: Progress in Natural Science, v. 16, p. 614–623.

Zhang, W.T., Lu, Y.H., Zhu, Z.L., Qian, Y.Y., Lin, H.L., Zhou, Z.Y., Zhang, S.G., and Yuan, J.L., 1980, Cambrian trilobite faunas of southwestern China: Palaeontologica Sinica, new series B, v. 16, 497 p. [in Chinese]

Zhao, Y., Peng, S., Yuan, J.-L., Esteve, J., Yang, X., Wu, M., and Chen, Z., 2019, Bioestratigrafía a partir de trilobites de las Formaciones de Balang y "Tsinghsutung" (Serie Cámbrica 2, Piso 4) en el área de Balang, Jianhe, Guizhou, China meridional: Estudios Geológicos, v. 75, e119. https://doi.org/10.3989/egeol.43595.574.

Zhou, T.-M., Liu, Y.-R., Meng, X.-S., and Sun, Z.-H., 1977, Trilobita, *in* Geological Bureau of Henan Province, ed., Palaeontological Atlas of Central and South China. Guizhou (1): Beijing, Geological Publishing House, p 107–266. [in Chinese]